

**NASA TECHNICAL
MEMORANDUM**



NASA TM X-2657

NASA TM X-2657

**CASE FILE
COPY**

**AVERAGE HEAT-TRANSFER CHARACTERISTICS
OF A ROW OF CIRCULAR AIR JETS
IMPINGING ON A CONCAVE SURFACE**

by John N. B. Livingood and James W. Gauntner

Lewis Research Center

Cleveland, Ohio 44135

NATIONAL AERONAUTICS AND SPACE ADMINISTRATION • WASHINGTON, D. C. • OCTOBER 1972

1. Report No. NASA TM X-2657		2. Government Accession No.		3. Recipient's Catalog No.	
4. Title and Subtitle AVERAGE HEAT-TRANSFER CHARACTERISTICS OF A ROW OF CIRCULAR AIR JETS IMPINGING ON A CONCAVE SURFACE				5. Report Date October 1972	
				6. Performing Organization Code	
7. Author(s) John N. B. Livingood and James W. Gauntner				8. Performing Organization Report No. E-7015	
9. Performing Organization Name and Address Lewis Research Center National Aeronautics and Space Administration Cleveland, Ohio 44135				10. Work Unit No. 501-24	
				11. Contract or Grant No.	
12. Sponsoring Agency Name and Address National Aeronautics and Space Administration Washington, D. C. 20546				13. Type of Report and Period Covered Technical Memorandum	
				14. Sponsoring Agency Code	
15. Supplementary Notes					
16. Abstract <p>A study of the average heat-transfer characteristics of air jets impinging on the concave side of a right-circular semicylinder is reported. Results from existing correlations are compared with each other and with experimental heat-transfer data for a row of circular jets. Two correlations available in the literature are recommended for use in designing cooled turbine vanes and blades.</p>					
17. Key Words (Suggested by Author(s)) Literature survey Impinging jets Cylindrical surface Heat-transfer data				18. Distribution Statement Unclassified - unlimited	
19. Security Classif. (of this report) Unclassified		20. Security Classif. (of this page) Unclassified		21. No. of Pages 23	
				22. Price* \$3.00	

* For sale by the National Technical Information Service, Springfield, Virginia 22151

AVERAGE HEAT-TRANSFER CHARACTERISTICS OF A ROW OF CIRCULAR AIR JETS IMPINGING ON A CONCAVE SURFACE

by John N. B. Livingood and James W. Gauntner

Lewis Research Center

SUMMARY

A study of the average heat-transfer characteristics of air jets impinging on the concave side of a right-circular semicylinder is reported. Results from existing correlations are compared with each other and with experimental heat-transfer data for a row of circular jets.

These experimental data were for two different-size semicylindrical configurations: the small configuration consisted of a right-circular semicylinder 1.27 centimeters (0.5 in.) in diameter joined to two parallel plates; the large configuration consisted of a right-circular semicylinder 12.7 centimeters (5 in.) in diameter. A row of 12 holes 0.095 centimeter (0.0375 in.) in diameter and with center-to-center spacing of 6.67 hole diameters and hole-to-target separation distances of 13.33 and 26.67 hole diameters were considered for the small-configuration tests. For the large configuration, holes 0.318, 0.635, and 0.952 centimeter (0.125, 0.25, and 0.375 in.) in diameter and with center-to-center spacings of 2, 4, and 8 hole diameters and hole-to-target separation distances of 2, 5, and 8 hole diameters were considered.

The small-configuration data showed Nusselt numbers lower than those predicted from the correlations; this was attributed to the fact that the outer extremes of the small-configuration test surface are less likely to be impingement cooled than a right-circular semicylinder of the same cooled length used in the correlations. The large-configuration Nusselt numbers were higher than those predicted by most of the existing correlations; this was attributed to the interruption of the conduction path along the target surface as a result of the use and locations of calorimeters to measure the heat flux. Two correlations are recommended for use in future design of impingement-cooled turbine vanes and blades.

INTRODUCTION

The leading-edge region of an air-cooled turbine vane or blade is exposed to high heat flux; hence, this region requires effective cooling. The impingement of cool air on the inside surface is an excellent method to cool the leading-edge region of a gas turbine airfoil. The leading-edge region of a turbine vane or blade is often approximated as part of a semicylindrical surface for analytical and experimental models. Impingement-cooling research has been and is being conducted in the United States and abroad by using actual airfoils and semicylindrical models. The results of some of these investigations are reported in references 1 to 15. Generally, each investigator's results are limited to particular geometrical configurations and prescribed ranges of variables. This report presents and compares the heat-transfer characteristics obtained from existing impingement-cooling correlations and presents additional data to further evaluate the various correlation methods.

In the present investigation, average heat-transfer data were obtained for two different-size semicylinders. The smaller semicylinder had a diameter of 1.27 centimeters (0.5 in.). The convex surface of the smaller semicylinder was electrically heated by wires that were brazed to the surface. The larger semicylinder had a diameter of 12.7 centimeters (5.0 in.) and its convex surface was steam heated.

For the smaller configuration, a single row of 12 circular orifices 0.095 centimeter (0.0375 in.) in diameter and with center-to-center spacings of 13.33 and 26.67 hole diameters were investigated. For the large semicylinder, circular orifices 0.318, 0.635, and 0.952 centimeter (0.125, 0.250, and 0.375 in.) in diameter and with center-to-center spacings of 2, 4, and 8 diameters and orifice-to-target spacings of 2, 5, and 8 diameters were investigated. Reynolds numbers ranging from about 200 to 12 000 were considered.

The data presented herein were obtained at the Newark College of Engineering under contract with NASA (Contract number NAS3-11175). Drs. Hrycak and Chen supervised the experimental work at the Newark College of Engineering.

SYMBOLS

- A nozzle flow area
- A_c cross-sectional area of calorimeter
- b equivalent slot width, $\pi d_n^2 / 4c_n$
- C_D discharge coefficient
- c_n nozzle center-to-center spacing

c_p	specific heat
D	cylinder diameter
D_{eff}	effective cylinder diameter, $\pi D_{\text{eff}}/4 = l$
d_h	hydraulic diameter, $2bc_n(n-1)/[b+c_n(n-1)]$
d_n	nozzle diameter
\bar{h}	average heat-transfer coefficient
k	thermal conductivity
l	cooled target length measured from stagnation line
\overline{Nu}_b	average Nusselt number, $\bar{h}b/k$
n	number of nozzles
Pr	Prandtl number, $c_p\mu/k$
Re_b	Reynolds number (based on nozzle exit velocity and equivalent slot width)
$Re_{b,a}$	Reynolds number (based on arrival velocity and equivalent slot width)
T	temperature
V	nozzle exit velocity
V_a	arrival velocity
\dot{w}	flow rate
x	coordinate along axis of calorimeter
z_n	nozzle-to-target separation distance
μ	viscosity

SURVEY OF PREVIOUS WORK

Professor Metzger and his associates at Arizona State University have been actively working in impingement cooling; references 1 to 5 present some of the results of this work. Rows of circular jets and slot jets impinging on concave semicylindrical surfaces were studied. For circular jets with spacing-to-diameter ratios from 1.67 to 6.67, maximum cooling was achieved when the row of jets was located about 1 nozzle diameter from the target surface. For slot jets, maximum cooling occurred when the slot jets were about 3 slot widths from the target surface (ref. 2). Metzger has studied the effects on the heat-transfer coefficients of variations in the ratio of nozzle spacing to nozzle diameter c_n/d_n , the ratio of cooled target length to equivalent slot width l/b ,

the ratio of nozzle-to-target separation distance to equivalent slot width z_n/b , and Reynolds number. Correlations resulting from these studies for targets with half-angles of 10° , 20° , 30° , 45° , 60° , and 90° (for conditions of optimum nozzle-to-target separation distance) are presented in table I. These correlations are used in this report. The ranges of the parameters on which these correlations were based are also shown in table I. The effects of leading-edge sharpness and of elongation of the leading edge are discussed in reference 5.

An investigation of round-jet impingement on a concave semicylindrical surface was reported in reference 6. Reference 6 correlates average heat-transfer data from a flat plate and for two semicylinders by basing the dimensionless parameters on twice the target surface length, $2l$, and by use of the arrival velocity in the Reynolds number. (The arrival velocity, defined as the jet velocity at the test surface if the test surface did not exist, was obtained from the relation $V_a/V = 6.63/(z_n/d_n)$.) The correlation is given in table I in the current nomenclature.

Another investigation of impingement cooling of concave semicylindrical surfaces is in progress at the University of Cincinnati under the supervision of Professor Tabakoff. Some results of these studies appear in references 7 to 10. Reference 7 presents an analytical method for predicting the heat transfer from a slot to a semicylindrical surface in the stagnation region, the transition region, and the wall jet region. Predicted and experimental heat-transfer coefficients agreed in the stagnation region; elsewhere, the predicted values exceeded the experimental results. Reference 8 reports experimental results for impingement from a row of circular jets and presents a correlation equation for the average Nusselt number (table I). Reference 9 reports results of experiments for a slot jet, a row of circular jets, and an array of circular jets. Test results from arrays of round jets are reported in reference 10, where it is shown that arrays of holes give higher average heat-transfer coefficients than a single row of holes.

Experimental data on impingement cooling of a full-scale plastic model of the inside leading-edge region of a turbine airfoil are reported in reference 11. Local heat-transfer coefficients were obtained by considering Joulean dissipation in very thin spanwise platinum strips bonded to the model at various chordwise positions; spanwise average coefficients were obtained. Both stagnation line and average data were successfully correlated in terms of the dimensionless quantities d_n/c_n , d_n/D , and z_n/d_n for a range of nozzle diameters, center-to-center spacings, and two leading-edge-region diameters. The average Nusselt number, the correlation of which is given in table I, was found to decrease exponentially with increasing z_n/d_n .

Another investigation, for a single nozzle diameter, a single center-to-center spacing, and a single leading-edge-region diameter is reported in reference 12. Average heat-transfer data were correlated on an equivalent slot basis. This correlation contains a term accounting for the angle of the jet exhaust hole and includes a discharge coefficient in the Nusselt number (table I). Reference 12 concluded that jet impingement

TABLE I. - CORRELATIONS

Correlation number	Reference	Correlation	Ratio of cylinder to nozzle diameter, D/d_n	Ratio of nozzle spacing to nozzle diameter, c_n/d_n	Ratio of nozzle to target separation distance to nozzle diameter, z_n/d_n	Ratio of nozzle to target separation distance to equivalent slot width, z_n/b	Ratio of cooled surface target length to equivalent slot width, l/b	Reynolds number, Re_b
1	2	$Nu_b = \frac{0.355}{2^{0.27}} Pr^{0.52} \left(\frac{b}{l}\right) Re_b^{0.73}$	8.33	1.67 to 6.67		2 to 35	4.7 to 55.6	575 to 3150
2	3	$Nu_b = 0.87 Pr^{0.475} \left(\frac{b}{l}\right) \left(\frac{b}{d_n}\right)^{0.386} Re_b^{0.614}$	8.33	1.67		1 to 15	1.6 to 14	875 to 3150
3	3	$Nu_b = 0.2 Pr^{0.504} \left(\frac{b}{l}\right) \left(\frac{b}{d_n}\right)^{0.208} Re_b^{0.792}$	8.33	6.67		4 to 15	6.2 to 36.9	700 to 2500
4	6	$Nu_b = 0.36 \left(\frac{b}{2l}\right)^{0.38} Re_b^{0.62}$	3.6	3.3	1.8 to 7.3	15.5	12.2	2300 to 41 000
5	8	$Nu_b = 0.813 \left(\frac{d_n}{D_{eff}}\right)^{0.79} \left(\frac{d_n}{c_n}\right)^{0.126} \left(\frac{d_n}{z_n}\right)^{0.0135} \left(\frac{b}{2l}\right)^{0.285} Re_b^{0.715}$	9.7 to 11.7	2.4 to 4.9	2 to 5.8	6 to 36.3	23.6 to 56.4	1800 to 41 000
6	11	$Nu_b = 0.63 \left(\frac{b}{d_n}\right)^{0.3} \left(\frac{d_n}{c_n}\right)^{0.5} \left(\frac{d_n}{D}\right)^{0.6} \times \left\{ \exp \left[-1.27 \left(\frac{z_n}{d_n}\right) \left(\frac{d_n}{c_n}\right)^{0.5} \left(\frac{d_n}{D}\right)^{1.2} \right] Re_b^{0.7} \right\}$	1.54 to 15.6	4 to 15.6	1.0 to 16	0.35 to 700	20 to 180	300 to 2000
7	12	$Nu_b = 0.03 Pr^{1/3} \left(\frac{z_n}{b}\right)^{-0.4} Re_b^{0.7} C_D^{-1}$	12.5	5	7.5 to 20	49 to 129	294	1000 to 6000
8	14	$Nu_b = 0.26 \left(\frac{b}{d_n}\right)^{0.35} Re_b^{0.65} \left(\frac{z_n}{b}\right)^{-0.22}$ for $\frac{z_n}{b} > 7$				7 to 13	7.3 to 12.2	2000 to 50 000
9	14	$Nu_b = 0.17 \left(\frac{b}{d_n}\right)^{0.35} Re_b^{0.65}$ for $\frac{z_n}{b} \geq 7$				1.5 to 7	2 to 7.3	2000 to 50 000

in a closed cavity is affected to a lesser degree by the nozzle-to-target spacing than for a flat plate because of recirculation currents in the closed cavity.

Burggraf (ref. 13) investigated impingement from a row of circular jets into a cavity, with the spent flow exiting either from only one side or from both sides of the cavity. On the no-discharge side, the flow recirculated; and on the discharge side, there was an acceleration of flow, which increased the heat-transfer adjacent to the discharge holes.

The results of a Russian experimental investigation of impingement cooling of a parabolically shaped passage are reported by Dyban and Mazur (ref. 14). Local heat-transfer coefficients measured in their investigation exhibited a U-shaped curve with a minimum at the stagnation line and two peaks located at a given distance from the stagnation line. This U-shaped distribution was not found in any of the other references mentioned. Correlations of local heat transfer and of the average heat transfer between peaks were obtained for the ranges of the variables considered. (It is also noted in the reference that the ratio of the diameter of the circle inscribed in the concave surface to the width of the passage could affect both the local and average heat transfer.) Table I contains the average correlation.

Some preliminary test results on impingement cooling of a turbine vane leading-edge region are presented in reference 15. The results show that impingement cooling is superior to convection cooling through radial holes with the same cooling airflow.

APPARATUS AND PROCEDURE

A schematic diagram of the apparatus is shown in figure 1. Air supplied by a compressor flowed through a filter and oil separator into a large storage tank to provide a steady flow. From the storage tank the air flowed through an inlet tank connected to four rotameters in parallel. Depending on flow rate, the flow was routed through a selected rotameter and into a tube connected to a plenum chamber. The air flowed through two flexible hoses from the plenum chamber into another chamber which contained the row of nozzles through which the air passed to impinge on the test cylinder surface. The test section was secured to a stand made from a grinding machine bed, which permitted an accurate alignment of the test section and the nozzle chamber.

The rotameters were calibrated within an error of less than 1 percent of full scale. The air pressure in the rotameter was measured at the inlet of the rotameter with a Bourdon-type pressure gage. (The inlet valve of the rotameter was kept fully open, and the flow was controlled by adjusting the outlet valve of the rotameter.) The temperature of the air in the rotameter was measured by a thermocouple placed in the pipe near the rotameter outlet.

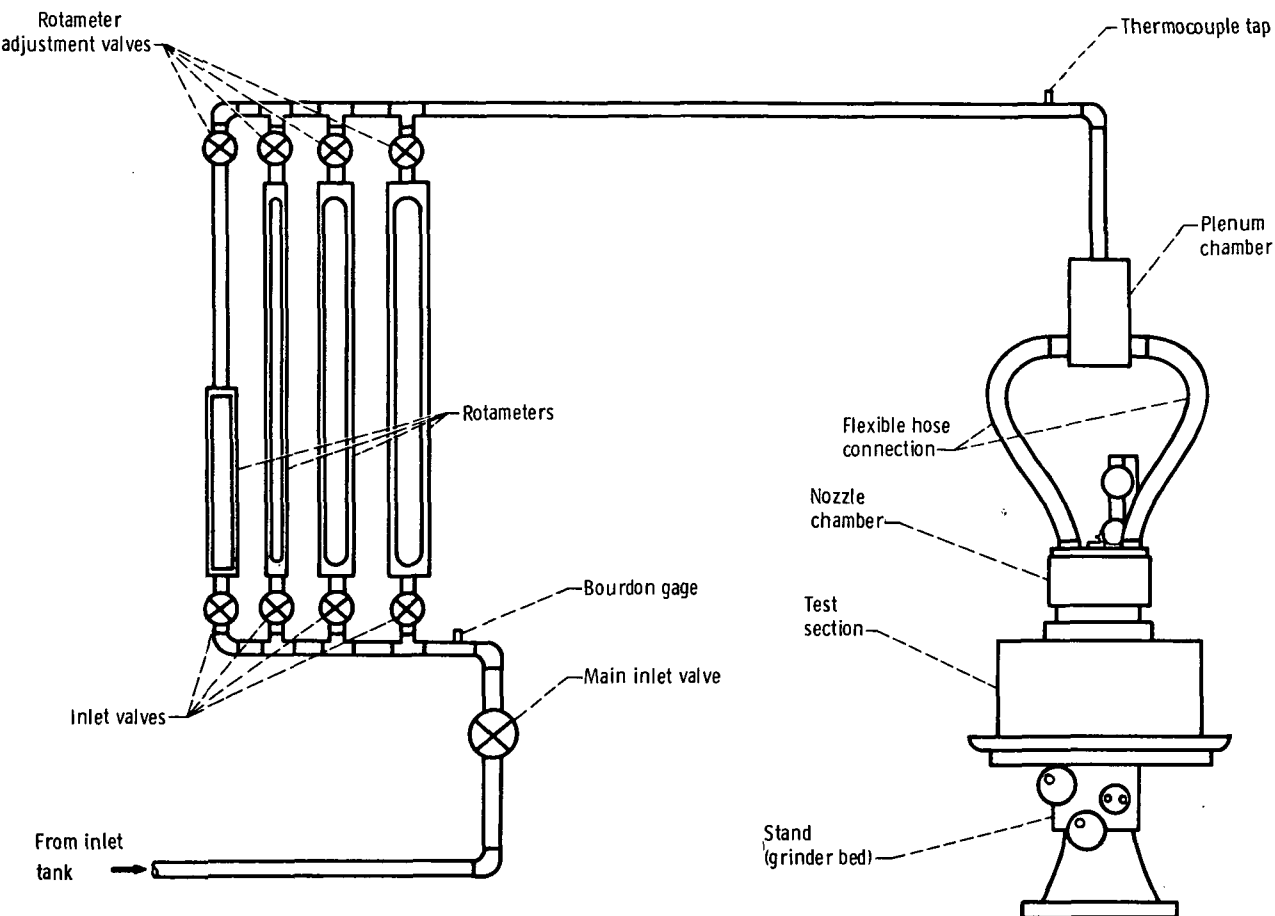
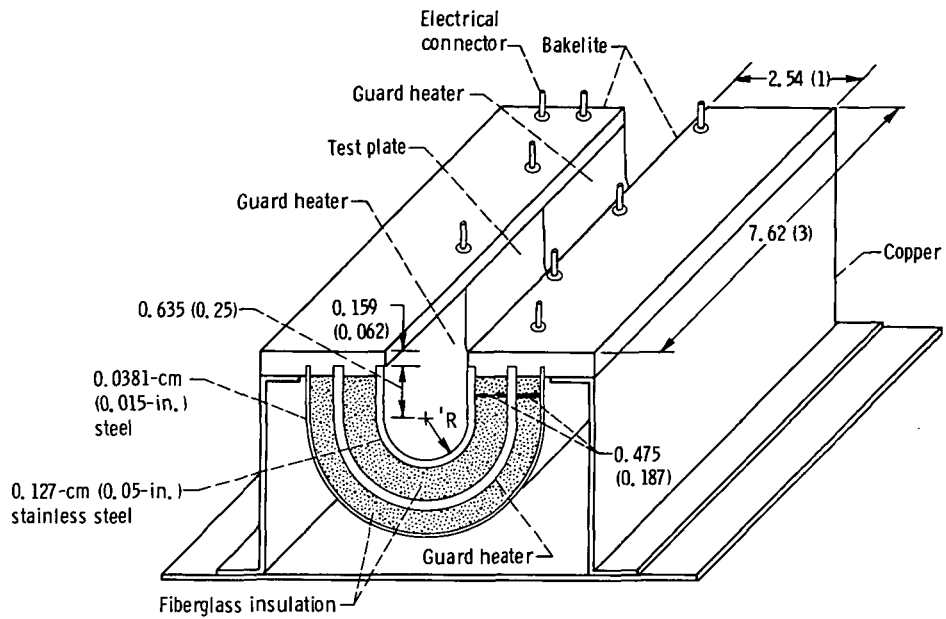


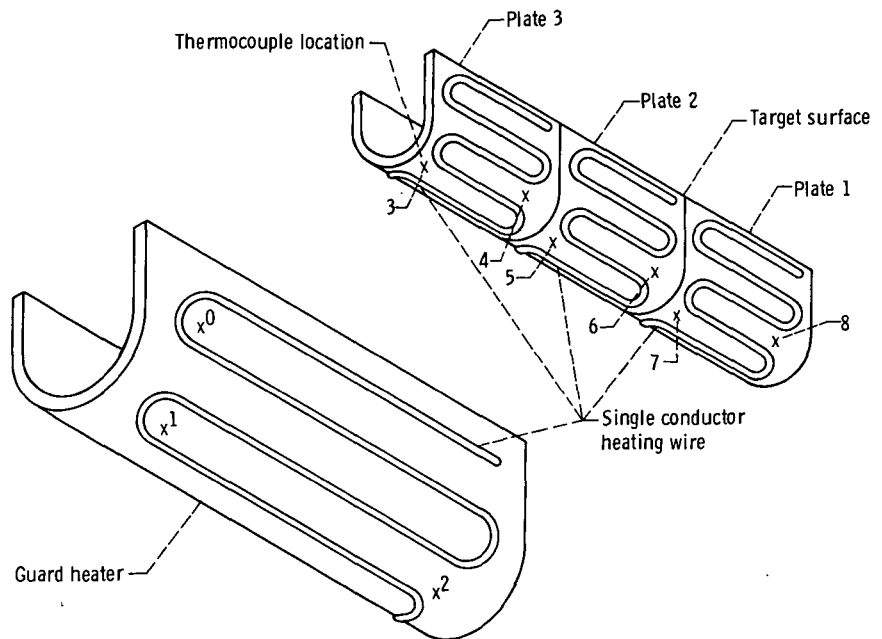
Figure 1. - Schematic of test apparatus.

Small-Scale Configuration

A diagram of the small-scale test surface and guard heaters is shown in figure 2(a). The concave test surface and guard heaters consisted of a semicylindrical surface 1.27 centimeters (0.5 in.) in diameter extended on either side by two parallel plates 0.635 centimeter (0.25 in.) long. These semicylindrical surfaces were made from a 2.54-centimeter (1-in.) plate that was 0.127 centimeter (0.05 in.) thick. On the convex side of the target surface was a 0.475-centimeter (0.187-in.) thick layer of fiberglass insulation, a 0.127-centimeter (0.05-in.) thick stainless-steel guard heater, another 0.475-centimeter (0.187-in.) thick layer of fiberglass insulation, and a 0.0381-centimeter (0.015-in.) steel outer casing. Heating wires were soldered to the three-plate target surface and the outer guard heater, as shown in figure 2(b). The center plate of the target surface (plate 2) was heated to a temperature of 9.5 to 14 K (17° to



(a) Test surface and guard heaters.



(b) Heating wire and thermocouple locations on target surface and guard heater.

Figure 2. - Test section for small-scale concave configuration. (Dimensions are in cm (in.).)

TABLE II. - NOZZLE CONFIGURATIONS CONSIDERED

Case	Nozzle diameter, d_n		Nozzle center-to-center spacing, c_n		Nozzle-to-target separation distance, z_n		Cooled surface length from stagnation line, l		Equivalent slot width, b		Ratio of nozzle spacing to nozzle diameter, c_n/d_n		Ratio of nozzle-to-target separation distance to nozzle diameter, z_n/d_n		Ratio of cooled surface length to equivalent slot width, l/b		Ratio of nozzle-to-target separation distance to equivalent slot width, z_n/b		Ratio of equivalent slot width to nozzle diameter, b/d_n	
	cm	in.	cm	in.	cm	in.	cm	in.	cm	in.										
Small-scale configuration																				
1	0.095	0.0375	0.635	0.25	1.270	0.5	1.632	0.6427	0.0112	0.0044	6.67	13.33	145	113	0.1180					
2	.095	.0375	.635	.25	2.540	1.0	1.632	.6427	.0112	.0044	6.67	26.67	145	226	.1180					
Large-scale configuration																				
3	0.318	0.125	2.54	1.0	0.635	0.25	9.975	3.927	0.0312	0.0123	8	2	319	20	0.0982					
4			2.54	1.0	1.588	.625			.0312	.0123	8	5	319	51	.0982					
5			2.54	1.0	2.540	1.0			.0312	.0123	8	8	319	82	.0982					
6			1.27	0.5	0.635	0.25			0.0622	0.0245	4	2	160	10	0.1963					
7			1.27	.5	1.588	.625			.0622	.0245	4	5	160	26	.1963					
8			1.27	.5	2.540	1.0			.0622	.0245	4	8	160	41	.1963					
9			0.635	0.25	0.635	0.25			0.1247	0.0491	2	2	80	5	0.3928					
10			.635	.25	1.588	.625			.1247	.0491	2	5	80	13	.3928					
11			.635	.25	2.540	1.0			.1247	.0491	2	8	80	20	.3928					
12	0.635	0.25	5.08	2.0	1.270	0.5			0.0622	0.0245	8	2	160	20	0.0982					
13			5.08	2.0	3.175	1.25			.0622	.0245	8	5	160	51	.0982					
14			5.08	2.0	5.080	2.0			.0622	.0245	8	8	160	82	.0982					
15			2.54	1.0	1.270	0.5			0.1247	0.0491	4	2	80	10	0.1963					
16			2.54	1.0	3.175	1.25			.1247	.0491	4	5	80	26	.1963					
17			2.54	1.0	5.080	2.0			.1247	.0491	4	8	80	41	.1963					
18			1.27	0.5	1.270	0.5			0.2494	0.0982	2	2	40	5	0.3928					
19			1.27	.5	3.175	1.25			.2494	.0982	2	5	40	13	.3928					
20			1.27	.5	5.080	2.0			.2494	.0982	2	8	40	20	.3928					
21	0.952	0.375	7.62	3.0	1.905	0.75			0.0935	0.0368	8	2	107	20	0.0982					
22			7.62	3.0	4.763	1.875			.0935	.0368	8	5	107	51	.0982					
23			7.62	3.0	7.620	3.0			.0935	.0368	8	8	107	82	.0982					
24			3.81	1.5	1.905	0.75			0.1869	0.0736	4	2	53	10	0.1963					
25			3.81	1.5	4.763	1.875			.1869	.0736	4	5	53	26	.1963					
26			3.81	1.5	7.620	3.0			.1869	.0736	4	8	53	41	.1963					
27			1.905	0.75	1.905	0.75			0.3741	0.1473	2	2	27	5	0.3928					
28			1.905	.75	4.763	1.875			.3741	.1473	2	5	27	13	.3928					
29			1.905	.75	7.620	3.0			.3741	.1473	2	8	27	20	.3928					

25° F) above room temperature with a 12-volt dc battery and was used to evaluate the heat-transfer rate. The other plates (plates 1 and 3) and the guard heater were heated with the 115-volt ac supply through small transformers to the same temperature as plate 2 to eliminate end effects and the transfer of heat from plate 2 to the surroundings. Nine copper constantan thermocouples were used to measure the target surface and guard heater temperatures (fig. 2(b)). In order to eliminate spent flow along the axis of the semicylinder, the target surface was blocked with smooth panels at both ends.

The line of nozzles impinging on the target surface was made from a 0.952-centimeter (0.375-in.) thick copper plate with 12 holes of 0.095-centimeter (0.0375-in.) diameter at a center-to-center spacing of 0.635 centimeter (0.25 in.). The target was mounted on a grinding machine stand and positioned at distances of 1.27 and 2.54 centimeters (0.5 and 1 in.) from the impinging nozzles. Cases 1 and 2 in table II summarize the geometrical dimensions associated with the small-scale configuration.

Large-Scale Configuration

The large-scale concave semicylindrical target was made from a section of a 12.7-centimeter (5-in.) diameter 304-stainless-steel pipe. The target surface was 25.4 centimeters (10 in.) in length and had a nominal wall thickness of 1.143 centimeters (0.45 in.). Both ends of the target surface were blocked with Plexiglass side walls. The convex surface was steam heated by placing it over a small tank in which water was kept boiling, as shown in figure 3(a). In order to eliminate some of the heat transfer from the exhaust air to the air in the nozzle chamber, reflective insulation over a layer of flannel fabric was attached to the nozzle chamber. Several layers of plastic air filter material were inserted over an expanded aluminum screen in the nozzle plenum to achieve a uniform distribution of air.

Twenty-one heat calorimeters were attached to a brass support plate and were insulated from the target surface by means of a 0.159-centimeter (0.0625 in.) air gap, as shown in figure 3(b). The calorimeters were made from the same kind of stainless steel as the target surface and were in the shape of cylinders 0.508 centimeter (0.2 in.) in diameter and 1.143 centimeter (0.45 in.) long with two thermocouples installed 1.016 centimeters (0.40 in.) apart. Thermal conductivity data were obtained by the National Bureau of Standards from calibration tests of a sample of the material. With this information, experimental heat flux through the calorimeter, $kA_c(dT)/(dx)$, could be calculated. The calorimeters were located at three spanwise positions, at 2.54-centimeter (1-in.) spacings; each spanwise position had a calorimeter located at the stagnation line and at 15°, 45°, and 75° on either side of the stagnation line. Figure 4 shows a calorimeter used to measure the heat flux through the test plate.

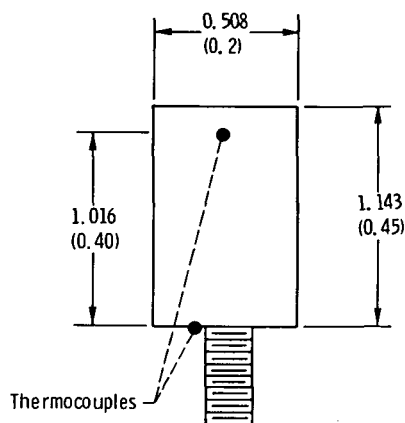


Figure 4. - Calorimeter used to measure heat flux.
(Dimensions are in cm (in.)).

Nozzles 0.318, 0.635, and 0.952 centimeter (0.125, 0.25, and 0.375 in.) in diameter with center-to-center spacings of 2, 4, and 8 nozzle diameters were investigated. The target was mounted on a grinding machine stand which permitted variations in the nozzle-target distance of 2, 5, and 8 nozzle diameters. Cases 3 to 29 in table II summarize the geometrical dimensions associated with the large-scale configuration. For each nozzle configuration and nozzle-to-target spacing, data were recorded at four different values of flow rate (Reynolds number). Then the nozzle-to-target spacing was increased and the process repeated.

RESULTS AND DISCUSSION

Experimental heat-transfer data for the small-scale configuration when the row of twelve 0.095-centimeter (0.0375-in.) diameter nozzles were located at a nozzle-to-target distance of 1.27 centimeters (0.5 in.) are listed as case I in table III and shown as the circles in figure 5(a). The figure shows a plot of average Nusselt number against Reynolds number, both variables being based on the equivalent slot width. The equivalent slot width is the width of a slot whose length is the center-to-center nozzle spacing and whose flow area is the same as the area of one of the circular nozzles; this permits comparison of impingement-cooling results obtained from either slots or nozzles. Also shown on figure 5(a) are a series of lines representing correlations proposed by other investigators, in which the geometrical values of the present configuration were inserted.

Although at first glance it appears that there is a rather large discrepancy between

TABLE III. - HEAT-TRANSFER DATA

[Reynolds number Re_b and Nusselt number Nu_b based on nozzle exit velocity and equivalent slot width.]

Case	Re _b	Nu _b	Case	Re _b	Nu _b	Case	Re _b	Nu _b	Case	Re _b	Nu _b	Case	Re _b	Nu _b			
1	137	0.347	7	5 260	8.39	12	285	1.32	18	11 911	27.2	24	4770	20.8			
	280	.541		5 257	8.03		262	1.33		11 808	27.7		2578	13.5			
	304	.620		2 617	5.83		623	2.35		5 154	20.7		2568	13.6			
	452	.901		2 619	5.85		604	2.33		5 142	20.8		1312	9.17			
	489	.764		1 256	3.82		1261	3.87		2 551	14.5		1298	9.15			
	553	.910		1 256	3.82		1261	3.86		2 555	14.6		460	4.26			
	630	.976		536	2.71		2640	5.12		959	8.30		424	4.19			
	638	.957		544	2.69		2623	5.70		952	8.30		4712	18.9			
	694	1.046											4728	19.2			
	1052	1.533		8	5 231		8.79	13		2691	6.22		19	11 700	31.3	25	527
1100	1.580	5 131	8.80		2669	6.27	8 276		29.7	2577	13.5						
1382	1.877	2 576	6.39		1333	4.11	5 147		24.0	2569	13.6						
1732	2.012	2 576	6.39		590	2.59	5 043		24.1	1311	8.80						
2014	2.467	1 235	4.02		575	2.65	2 610		15.9	1304	8.76						
		1 235	4.13		337	1.80	2 613		16.0	4741	18.9						
		569	2.67		309	1.77	1 034		8.97	4737	18.9						
		558	2.66				1 017		8.92	531	5.15						
		9	8 842		17.7	14	262		1.55	20	12 843	29.8		26	2533		13.4
			8 838		17.7		252		1.53		12 967	29.5			2509		13.5
			5 075	13.4	606		2.53	5 161	22.1		1290	8.80					
			5 047	13.4	584		2.52	5 132	22.1		1280	8.99					
			2 557	9.38	1333		3.97	2 603	15.0		551	5.00					
			2 557	9.38	1333		3.98	2 592	15.1								
			1 096	5.78	2697		6.38	1 060	7.99		27	5032	31.2				
			1 116	5.70	2697		6.35	1 060	7.99			5032	31.9				
			10	8 842	20.4		15	552	3.73			21	2 652		8.81	2619	21.1
				8 842	20.4			479	3.20				2 634		8.77	2612	21.1
		4 902		15.4	1261	6.19		1 336	6.29	1078			11.4				
		4 501		15.4	1242	6.29		1 328	6.24	8202			43.8				
		2 467		10.5	2569	9.31		627	4.07	8310			45.0				
		2 455		10.5	2567	9.33		593	3.99								
		1 108		6.23	5275	13.86		286	1.99	28			4906	31.6			
		1 100		6.24	5279	14.04		253	1.93				4907	31.2			
		11		1 061	6.08	16		538	3.75		22		2 625	9.76	2621	21.3	
				2 376	10.3			522	3.70				2 629	9.63	2615	21.4	
			2 369	10.6	1258		6.00	1 335	5.86			1079	12.3				
			4 953	15.8	2610		8.27	1 320	5.85			1055	12.6				
			4 934	15.4	2595		8.17	654	4.10			29	8047	42.1			
			12 165	23.1	5277		13.80	632	4.08				4883	33.5			
			8 909	21.4	5283		13.64	289	2.62				4884	33.6			
			8 838	21.2				282	2.53				2663	22.9			
			17				23	545	3.71	2668			8.65	2612	22.7		
								494	3.55				2 670	8.60	1074	13.0	
					1296	6.38		1 342	5.57		1053		13.2				
					1300	6.39		1 321	5.55								
					2669	9.23		660	3.67								
					5434	13.83		631	3.66								
								275	2.24								
								259	2.21								

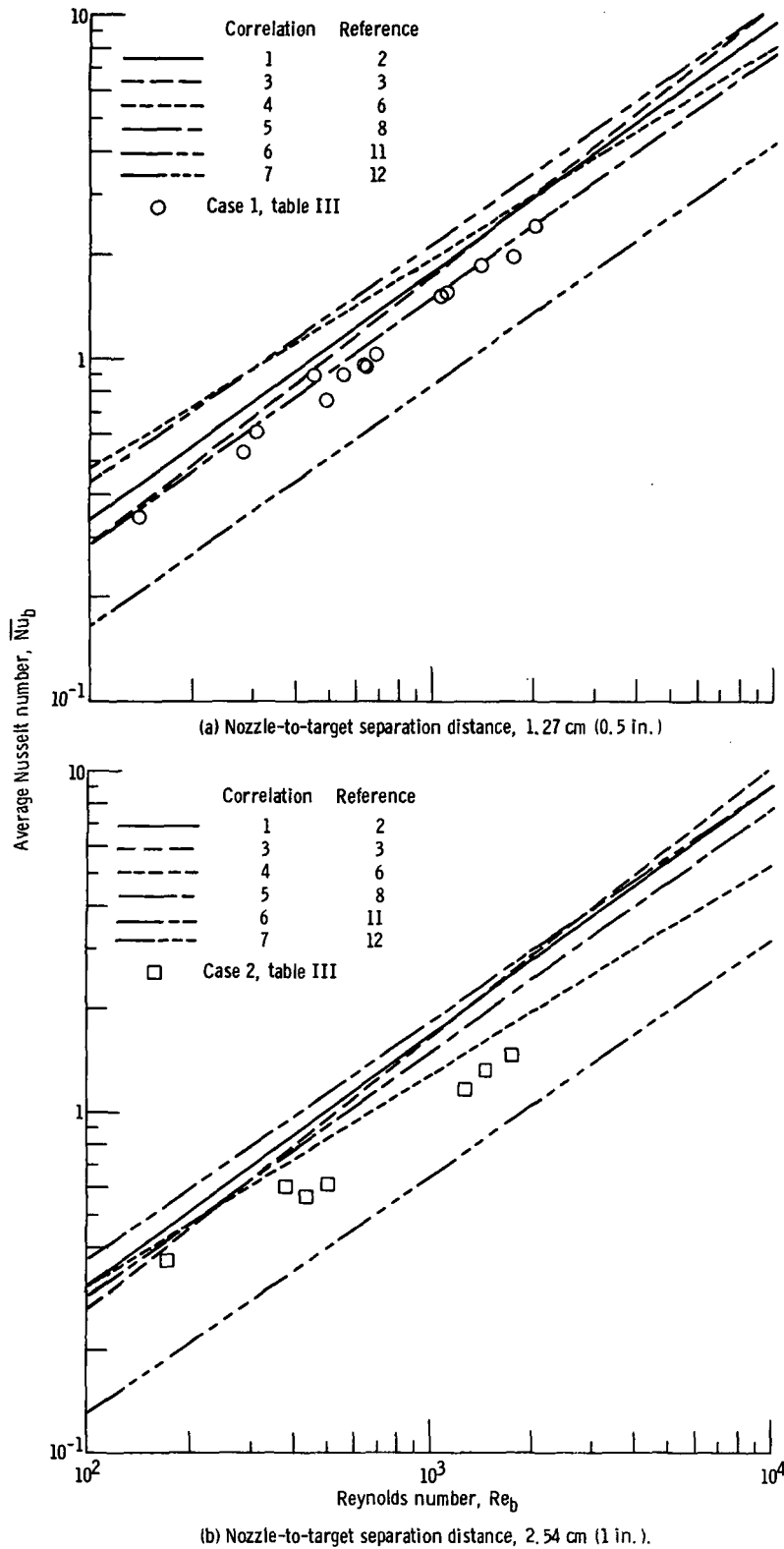


Figure 5. - Heat-transfer data from small-scale configuration compared with available correlations. Nozzle diameter, 0.095 cm (0.0375 in.); nozzle center-to-center spacing, 0.635 cm (0.25 in.); cylinder diameter, 1.27 cm (0.5 in.).

the data of this investigation and some of the correlations presented, it must be realized that the correlations resulted from investigations covering different configurations and ranges of variables. An attempt is made in the discussion which follows to point out these differences and to indicate what liberties were taken in applying the correlations to the present configurations.

Correlation (1) of table I was taken from reference 2, wherein an optimum nozzle target separation distance z_n/d_n of 1 was experimentally determined. The correlation was derived for nozzle diameters from 0.076 to 0.152 centimeter (0.03 to 0.06 in.), hole spacings from 1.67 to 6.67 nozzle diameters, and Reynolds numbers (based on equivalent slot width) to 3100. Values of l/b to about 55, with l determined for half-angles of 30° , 45° , 60° , and 90° , were considered. For the small-scale configuration reported herein, the nozzle diameter, nozzle spacing, and Reynolds number were within the preceding ranges; however, the l/b value was about double that of reference 2. It was estimated that the z_n/b effects could be accounted for by multiplying the \overline{Nu}_b calculated from correlation (1) by a correction factor of 0.75 obtained from figure 10 of reference 2.

Correlation (3) of table I, taken from reference 3, was empirically determined for a c_n/d_n of 6.67, identical to that for the small-scale configuration. Since this correlation arose from the same general conditions as correlation (1) and was made by the same investigators, correction as before for z_n/b effects yields essentially the same results as correlation (1).

Correlation (4) of table I, taken from reference 6, was obtained by using data from two semicylindrical test surfaces with 2:1 ratios of jet diameter, center-to-center spacing, equivalent slot width, and cooled target length. Nozzle-to-target distances as large as 8 nozzle diameters were considered; in this case, use of the arrival velocity in the Reynolds number accounted for this variation in nozzle-to-target distance. Figure 5(a) shows the correlation applied to the present configuration.

Correlation (5) of table I was taken from reference 8. Figure 5(a) shows this correlation, with the present geometrical factors inserted, to be in good agreement with the data reported herein. It should be noted that an effective semicylinder diameter D_{eff} was calculated from the semicylinder diameter and the parallel-plate extension length so that the cooled length used in the correlation would equal that of the experiment.

Correlation (6) of table I was taken from reference 11 and applied to the present case. The effective diameter D_{eff} was used in this correlation, as well as in correlation (5). The correlation was obtained for an actual vane leading-edge region; consequently, the nozzle diameters, center-to-center spacings, and target surface diameters were considerably smaller than those considered by the other investigators. However, reference 3 compares results obtained in the test reported therein with the correlation of reference 11 and found the latter to yield higher average Nusselt numbers than those

of reference 3 for all values of c_n/d_n . The same trend is shown in figure 5(a).

Correlation (7) of table I was taken from reference 12. In this application, a discharge coefficient of 0.60 was used (ref. 2). At present, there is no explanation as to why such low values of average Nusselt number were obtained. To make the correlation results agree with the data used, a much lower value of this discharge coefficient (of the order of 0.34) would have to be used; however, the assumed value of 0.60 appears to be a reasonable value, according to the available literature on discharge coefficients.

Figure 5(b) shows results similar to those of figure 5(a) for the small-scale configuration with the nozzle-to-target separation distance z_n of 2.54 centimeter (1 in.), double that of figure 5(a). A comparison of figures 5(a) and (b) clearly indicates that the data points in figure 5(b) are lower than those in figure 5(a); this is as expected since the nozzle-to-target separation distance for figure 5(b) is greater than that for figure 5(a). The discrepancies between correlation (4) and the data points in both figures are essentially the same because the use of the arrival velocity in the correlation accounts for the separation distance. Correlation (1), as noted in the discussion of figure 5(a), resulted from a consideration of optimum nozzle-to-target separation distance. Since the nozzle-to-target separation distance of figure 5(b) is twice that of figure 5(a), a greater extrapolation is necessary to correct for the nonoptimum z_n/b . The determination of a correction factor to account for the nozzle-to-target separation distance for correlation (1) in this case required an extremely large extrapolation of figure 10 of reference 2; the validity of such a large extrapolation is questionable. Correlation (6) gives the highest average Nusselt number, as in figure 5(a) and as reported in reference 3. The effect of the change in separation distance in correlation (5) is minimal, and correlation (5) is essentially the same in figures 5(a) and (b). Correlation (7), as before, is considerably below the data.

Tests of the small-scale configuration were made with only the nozzle-to-target separation distance being varied. Such variables as c_n , b , l , etc., which also affect the average Nusselt number, were not varied in these tests. As a consequence, a new correlation could not be developed from these test data.

Generally, the experimental average Nusselt numbers from the small-scale cylinder are lower than those predicted by the various correlations. This result seems reasonable since the correlations are for an average Nusselt number over one-half of a right-circular semicylinder, while the data are for an average over one-half of a right-circular semicylinder joined to two parallel plates. Although the length, as measured from the stagnation line, is the same for both the correlations and the data, the outer extremes of the test surface are less likely to be impingement cooled. Therefore, the average experimental Nusselt numbers for the data should be lower than those from the correlations.

Large-Scale Configuration

Figure 6 shows the average heat-transfer data for one series of runs for the large-scale configuration and compares the data with a number of existing correlations. The case selected (case 27, table III) was the one for the 0.952-centimeter (0.375-in.) diameter nozzle and a z_n/d_n of 2. Similar results were obtained for the other nozzle diameters and for the nozzle-to-target separation distances and center-to-center nozzle spacings considered. The large-scale data of figure 6 are considerably higher than those of the small-scale configuration. This may be attributed to the fact that the nozzle-to-target separation distance for the large-scale configuration is nearer the optimum; whereas, for the smaller-scale configuration the separation distance was more than 13 and 26 nozzle diameters for the data for figures 5(a) and (b), respectively. This variation in nozzle-to-target separation distance and the fact that the cooled length l was not scaled in the same ratio as the nozzle diameters and cylinder diameters were scaled makes it impossible to compare data from the two configurations.

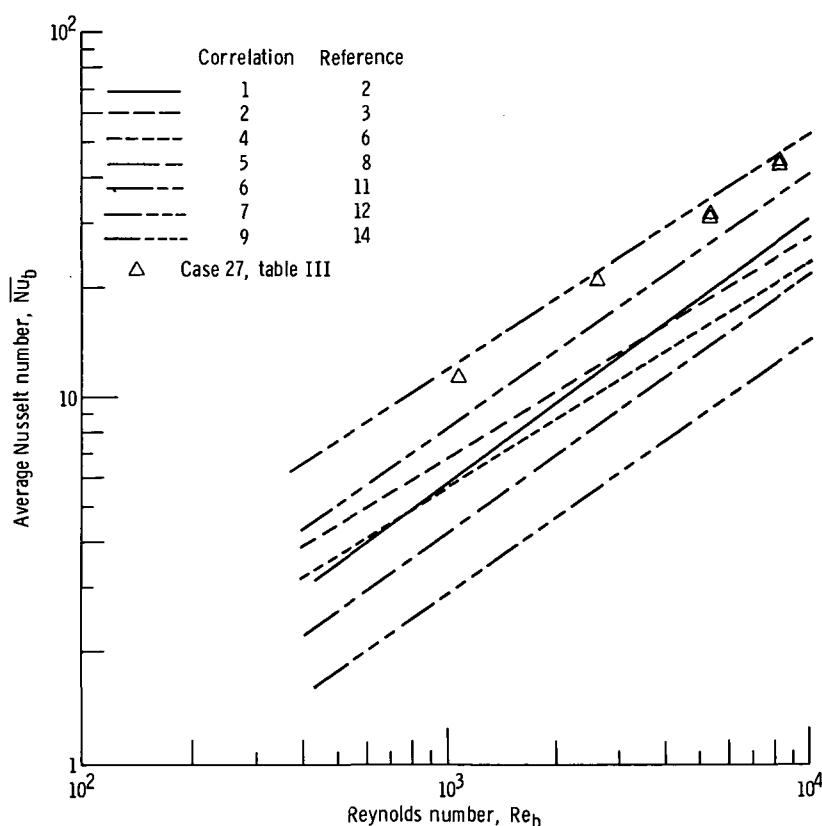


Figure 6. - Heat-transfer data for large-scale configuration compared with available correlations. Nozzle diameter, 0.952 cm (0.375 in.); nozzle center-to-center spacing, 1.905 cm (0.75 in.); cylinder diameter, 12.7 cm (5 in.); ratio of nozzle-to-target separation distance to nozzle diameter, 2.

The data in figure 6 are higher than most of the correlations, a condition opposite to that for the small-scale configuration. The heat flux was obtained for the large-scale configuration with the use of calorimeters. These were located as shown in figure 3. The presence of calorimeters interrupted the conduction path in the present experiments. This would result in higher local temperatures than if conduction were not interrupted and, therefore, also in higher average Nusselt numbers. Thus, a plausible reason exists for the data to be high and to exceed most of the correlations.

Correlation (9) in figure 6 was taken from reference 14, wherein a minimum Nusselt number was found at the stagnation line and peaks on either side of the stagnation line, a phenomenon not reported by other investigators of impingement on a concave surface. Correlation (9) resulted from averaging the Nusselt number between these two peaks. Therefore, correlation (9) should predict higher \overline{Nu} than those obtainable from data where the maximum Nusselt number was found at the stagnation line.

Figure 7 shows a plot of average Nusselt number against Reynolds number (cases 21, 24, and 27 of table III) for the 0.952-centimeter (0.375-in.) diameter nozzle with a fixed nozzle-to-target separation distance of 2 nozzle diameters and various center-to-center

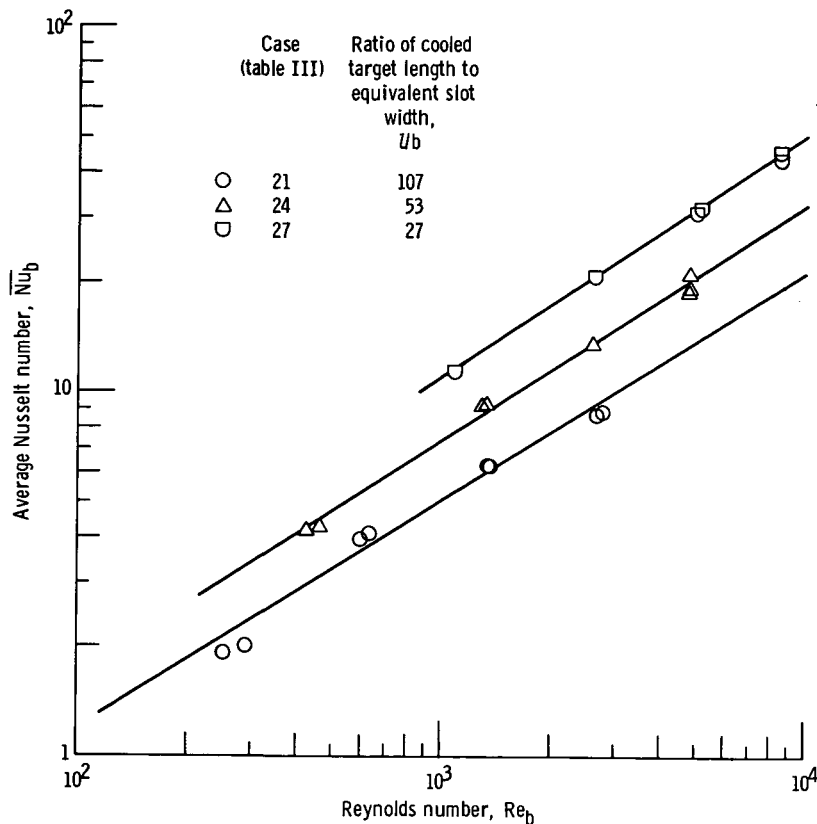


Figure 7. - Effect of ratio of cooled target length to equivalent slot width (or ratio of nozzle spacing to nozzle diameter) on average Nusselt number. Nozzle diameter, 0.952 cm (0.375 in.); ratio of nozzle-to-target separation distance to nozzle diameter, 2.

nozzle spacings (or equivalently, various values of l/b). The figure shows a monotonic decrease of average Nusselt number with increases in l/b for a fixed Reynolds number. This trend is in agreement with the results of reference 3. Similar trends were found for the other nozzles considered.

Figure 8 shows the effect of nozzle diameter on average Nusselt number for a nozzle-to-target spacing of 2 nozzle diameters and a center-to-center spacing of 2 nozzle diameters. The largest nozzle diameter furnished the highest average Nusselt numbers.

For the large-scale configuration, values of d_n , c_n , and z_n were varied (only l was held constant). However, careful inspection of the data indicated that systematic variations in the average Nusselt number were not obtained when these parameters were varied. Consequently, no attempt was made to develop a correlation of the large-scale-configuration experimental data.

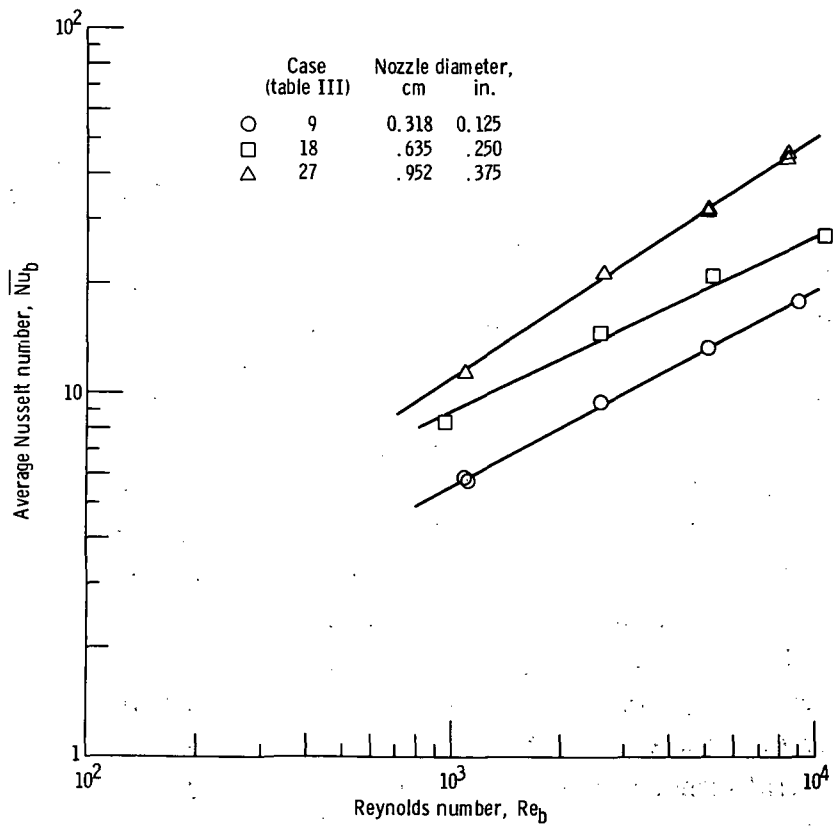


Figure 8. - Effect of nozzle diameter on average Nusselt number. Ratio of nozzle-to-target separation distance to nozzle diameter, 2; ratio of nozzle spacing to nozzle diameter, 2.

Recommended Correlation for Future Designs

A new correlation was not developed because of a lack of a sufficient amount of experimental data for the small-scale configuration and a lack of systematic trends in the data for the large-scale configuration. Therefore, one of the existing correlations will have to be used until additional experiments produce an improved one. Explanations for the discrepancies between the present data and the existing correlating lines were given in the discussions of figures 5(a), 5(b), and 6. Because discrepancies do exist, it is difficult to pinpoint which correlation should be used in future work.

If the geometrical dimensions are such that optimum spacing as suggested in reference 2 cannot be achieved, a correction factor estimated from information in reference 2 should be incorporated when applying correlation (1). Correlation (6) (ref. 11) contains a factor for the nozzle-to-target spacing, and gives average Nusselt numbers a bit higher than those of correlation (1) (ref. 2). It is recommended that either correlation (1) or (6) be used to design impingement-cooled vanes and blades until a better correlation becomes available.

CONCLUDING REMARKS

Although the experimental data reported herein for the average heat-transfer characteristics of air jets impinging on the concave side of a right-circular cylinder were not sufficient to permit the determination of a new correlation, they did serve as a basis for comparing existing correlations. The fact that the outer extremes of the small-scale test surface are less likely to be impingement cooled than are the outer extremes of a semicylinder of the same cooled accounts for the experimental Nusselt numbers being lower than those of correlation (1) even after a correction for separation distance was applied to the correlation. The variation in separation distance was so great that an extremely large extrapolation of information in reference 2 was used, and there is some doubt as to the validity of such an extrapolation. Although the large-scale configuration data showed higher Nusselt numbers than most of the correlations, a reason explaining these rather large discrepancies has been presented.

The fact that correlation (6) gave higher Nusselt numbers than correlation (1) confirms similar results already presented in reference 3. From the information reported herein, it appears that either correlation (1) or correlation (6) should be used in future design calculations.

The upper line on the large-scale-configuration results was obtained from reference 14. Reference 14 showed a minimum Nusselt number at the stagnation line and maximums on either side. None of the other investigators of impingement to a concave

surface reported such a phenomenon, although it had been reported for certain cases when a jet impinged on a flat plate. It appears that additional experiments of impinging jets (both single rows of holes and arrays of holes) on cylindrical surfaces are required in order to confirm the results of reference 14.

Lewis Research Center,
National Aeronautics and Space Administration,
Cleveland, Ohio, July 14, 1972,
501-24.

REFERENCES

1. Yamashita, Tamio: Heat Transfer Characteristics of Air Jets from Straight Line Arrays of Circular Nozzles Impinging on Concave Semi-Cylindrical Surfaces. MS Thesis, Arizona State Univ., 1968.
2. Metzger, D. E.; Yamashita, T.; and Jenkins, C. W.: Impingement Cooling of Concave Surfaces with Lines of Circular Air Jets. J. Eng. Power, vol. 91, no. 3, July 1969, pp. 149-158.
3. Jenkins, C. W.; and Metzger, D. E.: Local Heat Transfer Characteristics on Concave Cylindrical Surfaces Cooled by Impinging Slot Jets and Lines of Circular Jets with Spacing Ratios 1.25 to 6.67. Tech. Rep. ME-694, Arizona State Univ., May 1969.
4. Jenkins, Charles W.: Impingement Cooling of Concave Surfaces with Slot Jets and Single Lines of Circular Jets. MS Thesis, Arizona State Univ., 1969.
5. Metzger, D. E.; Baltzer, R. T.; and Jenkins, C. W.: Impingement Cooling Performance in Gas Turbine Airfoils Including Effects of Leading Edge Sharpness. Paper 72-GT-7, ASME, Mar. 1972.
6. Burggraf, F.: Average Heat Transfer Coefficients with a Row of Air Jets Discharging into a Half Cylinder. MS Thesis, Cincinnati Univ., 1967.
7. Clevenger, W.; and Tabakoff, W.: Investigation of the Heat Transfer Characteristics of a Two-Dimensional Jet Impinging on a Semi-Cylinder. Rep. THEMIS-AE-69-5, Cincinnati Univ. (AROD-T-4-10-E, AD-697165), Oct. 1969.
8. Ravuri, R.; and Tabakoff, W.: Heat Transfer Characteristics of a Row of Air Jets Impinging on the Inside of a Semicircular Cylinder. Rep. THEMIS-AE-71-18, Cincinnati Univ. (AROD-T-4-27-E, AD-718794), Jan. 1971.

9. Tabakoff, W.; and Clevenger, W.: Gas Turbine Blade Heat Transfer Augmentation by Impingement of Air Jets Having Various Configurations. J. Eng. Power, vol. 94, no. 1, Jan. 1972, pp. 51-60.
10. Tabakoff, W.; Ravuri, R.; and Clevenger W.: Heat Transfer by a Multiple Array of Round Jets Impinging Perpendicular to a Concave Surface. Rep. THEMIS-AE-71-20, Cincinnati Univ. (AROD-T-4-34-E, AD-727730), June 1971.
11. Chupp, Raymond E.; Helms, Harold E.; McFadden, Peter W.; and Brown, T. R.: Evaluation of Internal Heat-Transfer Coefficients for Impingement-Cooled Turbine Airfoils. J. Aircraft, vol. 6, no. 3, May-June 1969, pp. 203-208.
12. Jusionis, Vytautas J.: Heat Transfer from Impinging Gas Jets on an Enclosed Concave Surface. J. Aircraft, vol. 7, no. 1, Jan.-Feb. 1970, pp. 87-88.
13. Burggraf, F.: Local Heat Transfer Coefficient Distribution with Air Impingement into a Cavity. Paper 72-GT-59, ASME, Mar. 1972.
14. Dyban, Ye. P.; and Mazur, A. I.: Heat Transfer from a Flat Air Jet Flowing into a Concave Surface. Heat Transfer-Soviet Res., vol. 2, no. 3, May 1970, pp. 15-20.
15. Bassinot, E. C.: A Contribution to a Survey of Insert Vane Cooling. Paper 72-7, AIAA, Jan. 1972.

NATIONAL AERONAUTICS AND SPACE ADMINISTRATION
WASHINGTON, D.C. 20546

OFFICIAL BUSINESS
PENALTY FOR PRIVATE USE \$300

**SPECIAL FOURTH-CLASS RATE
BOOK**

POSTAGE AND FEES PAID
NATIONAL AERONAUTICS AND
SPACE ADMINISTRATION
451



POSTMASTER: If Undeliverable (Section 158
Postal Manual) Do Not Return

"The aeronautical and space activities of the United States shall be conducted so as to contribute . . . to the expansion of human knowledge of phenomena in the atmosphere and space. The Administration shall provide for the widest practicable and appropriate dissemination of information concerning its activities and the results thereof."

—NATIONAL AERONAUTICS AND SPACE ACT OF 1958

NASA SCIENTIFIC AND TECHNICAL PUBLICATIONS

TECHNICAL REPORTS: Scientific and technical information considered important, complete, and a lasting contribution to existing knowledge.

TECHNICAL NOTES: Information less broad in scope but nevertheless of importance as a contribution to existing knowledge.

TECHNICAL MEMORANDUMS: Information receiving limited distribution because of preliminary data, security classification, or other reasons. Also includes conference proceedings with either limited or unlimited distribution.

CONTRACTOR REPORTS: Scientific and technical information generated under a NASA contract or grant and considered an important contribution to existing knowledge.

TECHNICAL TRANSLATIONS: Information published in a foreign language considered to merit NASA distribution in English.

SPECIAL PUBLICATIONS: Information derived from or of value to NASA activities. Publications include final reports of major projects, monographs, data compilations, handbooks, sourcebooks, and special bibliographies.

TECHNOLOGY UTILIZATION PUBLICATIONS: Information on technology used by NASA that may be of particular interest in commercial and other non-aerospace applications. Publications include Tech Briefs, Technology Utilization Reports and Technology Surveys.

Details on the availability of these publications may be obtained from:

**SCIENTIFIC AND TECHNICAL INFORMATION OFFICE
NATIONAL AERONAUTICS AND SPACE ADMINISTRATION
Washington, D.C. 20546**